Ion pairs and their role in modulating stability of cold- and warm-active uracil DNA glycosylase.

Magne Olufsen[1], Elena Papaleo[2], Arne Oskar Smalås[1] & Bjørn Olav Brandsdal[1]*

[1]The Norwegian Structural Biology Centre, Department of Chemistry, University of Tromsø, N-9037 Tromsø, Norway.

[2]Department of Biotechnology and Bioscience, University of Milano-Bicocca, P.za della Scienza 2, 20126, Milan, Italy

*Corresponding author:
Bjørn Olav Brandsdal
Email: bjoerno@chem.uit.no
Phone: +47 77644057
Fax: +47 77644765

Running title: Ion pairs in cold- and warm-active UDG.
Key words: Uracil DNA glycosylase, salt-bridge, ion pairs, molecular dynamics simulations, stability, continuum electrostatics, cold adaptation,

Abstract

MD simulations and continuum electrostatics calculations have been used to study the observed differences in thermostability of cold- and warm-active uracil DNA glycosylase (UDG). The present study focuses on the role of ion pairs and how they affect the thermal stability of the two enzymes. Based on analysis of the MD generated structural ensembles, we find that cod UDG (cUDG) and human UDG (hUDG) have 11 and 12 ion-pairs which are present in at least 30 % of the conformations. The electrostatic contribution of the ion-pairs, computed using continuum electrostatics, is slightly more favorable in cUDG at 298 K. This is primarily attributed to more optimized interactions between the ion-pairs and nearby dipoles/charges in cUDG. When we take the environmental temperatures into account, the electrostatic stability becomes more favorable for the ion-pairs in the mesophilic enzyme. Both enzymes contain one three-member ionic network, but the one found in hUDG is far more stabilizing. Global salt-bridges are generally found to be more stabilizing than local bridges. In order to maintain structural integrity at low temperature, the electrostatic stability of ion-pairs is reduced, which possibly contribute to increased molecular flexibility at low temperature. Our results also suggest that care should be taken when performing statistical analysis of crystal structures with respect to ion-pairs, and that crystallization conditions must be carefully examined when performing such analysis.

Introduction

Life has evolved to cope with a broad range of different environments and is found in many extreme habitats such as low or high temperature niches, high pressure, low or high pH, high salinity etc. Adaptation to thermal extremes surely involves many mechanisms and survival in such environments requires enzymes with specific properties to maintain metabolism and reproductive activities. Interest in extremophilic enzymes has increased in the past years not only from an academic point of view but also as possible targets for commercialization. Cold-adapted, or so-called psychrophilic, enzymes are particularly attractive as targets due to their reduced thermal stability which is usually accompanied with an increased catalytic efficiency. The question of how enzymes can maintain stability in extreme environments continues to attract attention, and is presently not well understood. Much information about protein stability has been gained with the increasing availability of high-resolution structures and through comparative studies of homologous proteins[1,2]. Structural analysis of numerous psychrophilic, mesophilic and thermophilic enzyme homologues have revealed that their structures are often very similar[3], indicating difficulties with identifying features responsible for thermal adaptation by conventional methods. In an extensive study of structural differences between thermally adapted enzymes it was found that different protein families may use different strategies to adopt to low temperatures[4]. Psychrophilic enzymes often have decreased number of proline residues, increased number of glycine and acidic residues, low relative arginine ratio [arg/(arg+lys)] and lower content of ion pairs, aromatic interactions and/or hydrogen bonds compared to mesophilic counterparts[2,5-7]. There is also a trend that cold-adapted enzymes have increased interactions with solvent and higher accessibility to the active site[3,8], and multimeric psychrophilic enzymes often have decreased sub-unit interactions. It is clear that many different factors can contribute to enzymatic temperature adaptation and that no single factor can be invoked to explain adaptation in general.

Alteration of electrostatic interactions is one of the simplest ways nature can manipulate biophysical properties central to thermal stability, catalytic efficiency and substrate binding. It is clear that the stability of proteins stems from the delicate balance between opposing forces. The native folded three dimensional structure of proteins is only marginally stable and is at the edge of thermodynamic stability. Many different factors contribute to the overall stability of proteins, but the hydrophobic effect is generally accepted as the main contributor in protein folding. The hydrophobic effect drives the molecule towards a more condensed structure by minimizing unfavorable contacts between non-polar

residues and solvent. It is also accompanied by the entropically favorable release of water molecules around exposed hydrophobic groups[9-11]. In the initial phase of folding the hydrophobic effect leads to formation of the globular protein structure, often referred to as the molten globule state. The next step involves optimization of specific interactions that shifts the equilibrium towards the native state. Electrostatic interactions are an example of specific interactions and play an important role when a protein reaches its native fold. Other specific interactions that can contribute to the stability are van der Waals interactions and hydrogen bonds between polar groups[12,13]. Electrostatic interactions and their role in temperature adaptation of proteins is the key focus in this study.

There is at present only limited knowledge of how electrostatics is exploited by enzymes obtained from cold-adapted organisms. This is a result of the fact that only a few experimentally determined structures of psychrophilic enzymes are available. Enhanced electrostatic interactions has been found to play an important role in cold-adaptation of trypsin and uracil DNA glycosylase (UDG) with regard to activity[14-16], but the role in stability has not yet been investigated in detail. Cold active citrate synthase has strikingly different electrostatic potential in comparison to its hyperthermophilic counterpart, and focused electrostatic attraction of substrates has been proposed to be a possible source of the enhanced catalytic efficiency of the cold active citrate synthase[8]. Kumar and Nussinov[17] have also investigated the roles of electrostatics in psychrophilic, mesophilic and thermophilic citrate synthase using continuum electrostatics calculations. They found that electrostatics play different roles and appear to stabilize the thermophilic enzyme while ensuring proper protein solvation and active-site flexibility in the psychrophilic citrate synthase.

Salt-bridges or ion pairs can be considered as a special case of hydrogen bonds, and are composed of negative charges from Asp, Glu and C-terminals, and positive charges from Arg, His, Lys and N-terminals. These interactions are predominantly of electrostatic character and are also pH-dependent. Ionic interactions and their role in modulating protein stability have been the focus of many studies in the past two decades[9,18,19]. The increased occurrence of salt-bridges as well as salt-bridge networks in thermophilic proteins compared to their mesophilic homologues is the main reason for the great interest in electrostatics and its role in protein stability[20-22]. Even though the question of whether salt-bridges stabilize the native state of proteins has been raised repeatedly, no definite answer has yet been provided. Experimental and theoretical studies have showed that in some cases salt-bridges stabilize the native structure whereas in others an unfavorable contribution to protein stability is observed[9,23]. This is most likely related to the fact that the location, geometry and

optimization of the electrostatics varies greatly among not only homologous proteins but also between none-related proteins[23,24].

In order to improve our understanding of the role electrostatics play in adaptation to cold environments, uracil DNA glycosylase from cod (cUDG) and human (hUDG) is used as a comparative model system. UDG is an important enzyme in the DNA repair process and is the first enzyme in the base excision repair pathway, catalyzing the removal of promutagenic uracil residues from single- or double-stranded DNA[25]. The crystal structure of the catalytic domain of UDG from several species are known: human (hUDG)[26], Atlantic cod (cUDG)[27], virus 1[28], E.coli[29] and Epstein-barr virus[30]. The catalytic domain of hUDG and cUDG consists of 223 amino acids with a sequence identity of 75%, and the overall topology is a typical α/β protein[26]. High sequence and structural similarity makes UDG a good choice as a model system to explore adaptational features. Further support to this choice is also added by the fact that several crystal structures of mutant enzymes have been solved and subjected to kinetic and thermodynamic characterizations [16,27,31-34]. Moreover, UDG from Atlantic cod has been found to be up to ten times more catalytically active than the human counterpart between 283 and 310 K[32]. The psychrophilic cUDG has also been found to be much more pH and temperature labile than hUDG[31], indicating that cUDG is less stable compared to hUDG. The measured half-life was 0.5 min for cUDG and 8 min for hUDG at 323 K[32]. Even though these two enzymes has similar number of charged residues, similar amount of hydrogen bonds and no obvious differences in hydrophobic packing[27], the psychrophilic enzyme show less thermal stability compared to the mesophilic counterpart. Differences in salt-bridges are however observed in their respective crystal structures. The possible role of salt-bridges in thermal adaptation of UDG is in this study investigated using molecular dynamics simulation and continuum electrostatic calculations.

Methods

MD simulations

The AMBER8 program package[35] with the parm99 force field[36] was used to run and analyze the MD simulations. UDG contains several histidines and were with one exception (His148), considered as neutral in the simulations. This choice was based on existing data from NMR and continuum electrostatics calculations[37]. Water molecules were added to the protein with a 15 Å buffer from the edge of the box and described according to the TIP3P model[38]. The total box size for the system was approximately 85x70x75 Å with roughly 50 000 atoms in the system. Prior to the MD simulations, the molecular systems were subjected to 200 cycles of energy minimization of the water with the protein fixed and then 200 cycles of minimization of the whole system. In the initial phase the temperature of the system was slowly raised in steps to the final temperature of 300 K, followed by an equilibration period of 100 ps. The time step used was 2 fs and for every 1000 step, the rotational and translational motion was removed. In the production phase the simulation was run with the isothermal-isobaric ensemble (300 K and one atmosphere pressure). Pressure and temperature were maintained by the Berendsen coupling algorithm[39]. A 8 Å cutoff for non-bonded interactions was used in the simulation and the Particle-Mesh-Ewald (PME) method[40] was used to handle long-range interactions beyond the cutoff. SHAKE[41] was applied to constrain covalent bonds involving all hydrogen atoms. Coordinates were written to file every ps during the production phase, and the simulations were carried out for 5 ns for both cUDG and hUDG. The density, total energy, temperature and root-mean-square deviation plotted vs time were used to investigate the stability of the simulations, and all four properties are stable throughout the simulations (results not shown).

The accessible surface area (ASA) of the residues was calculated using WHAT IF[42], with the standard parameters. The ASA of a salt-bridge is the average ASA of the side chains of the two residues involved in the salt-bridge. The ASA was calculated for 10 snapshots from the MD simulations and the crystal structure, but only the average value is presented. The distances between salt-bridge partners were calculated with the AMBER software package. The distances were calculated between the following atoms: (Lys:Nζ, Arg:Cζ and His:Cε1) and (Asp:Cγ and Glu:Cδ). A cutoff of 5.0 Å was used to decide if the salt-bridge is stable with respect to distance. If two oppositely charged residues are within 5.0 Å for more than 30% of the simulation time it is considered to be a salt-bridge and the energy of the salt-bridge was calculated.

Continuum electrostatic calculations

Continuum electrostatic calculations were carried out on 99 structures from the MD simulations on hUDG and cUDG and on the crystal structure of these enzymes. Every 50th structure from the simulations was subjected to continuum calculations. The DelPhi program[43,44] was used to calculate the electrostatic stability of the salt-bridges. The calculations were performed using the partial charges and atomic radii of the AMBER force field (parm99)[36]. The PARSE3 set[45] of atomic radii was also tested together with the partial charges from the AMBER parm99 force field. On average the all AMBER parameter set stabilized each salt-bridge by 0.2 kcal/mol more than the mixed PARSE3 and the AMBER parameter set. Only the results from the all AMBER parameter set are shown. The electrostatics was calculated using the linear Poisson-Boltzmann equation and a grid size of 165x165x165 points in a 3-dimensional grid. Stepwise focusing was used to increase the accuracy[46]. Initially a rough grid was calculated with the Coulombic boundary conditions. The resulting grid of this calculation was adopted as the boundary condition for two further focused calculations, and in the last calculation the molecule occupied ~90% of the box. Lower boxfill values were also tested (~80%) but this gave similar results, consistent with published results[46]. A solvent probe of 1.4 Å was used to calculate the molecular surface. The dielectric constant of water is not constant with temperature, and the electrostatic energy was calculated for 0°C for the psychrophilic enzyme and 37°C for the mesophilic homologue. In addition, the electrostatic energy was calculated for both enzymes at 25°C. A bulk dielectric constant of 87.9, 80.0 and 75.9 was used for the temperatures 273 K, 298 K and 310 K, respectively. All the calculations were run both with 0.1 M salt and with zero ionic strength and three different dielectric constants of the protein were tested (4, 10 and 20).

The electrostatic stability of the salt-bridges has been calculated with respect to their corresponding hydrophobic isosteres[47]. The hydrophobic isosteres are the corresponding charged salt-bridge residues with all atom charges in the side chain set to zero[47]. The total electrostatic free energy of a salt-bridge ($\Delta\Delta G_{tot}$) can be divided into three terms:

Eq I: $$\Delta\Delta G_{tot} = \Delta\Delta G_{dslv} + \Delta\Delta G_{brd} + \Delta\Delta G_{prt}$$

The $\Delta\Delta G_{dslv}$ is the desolvation energy and in order to calculate this term, four DelPhi runs are needed: two of the folded protein with one of the salt-bridge side chain charged, and two calculations of the unfolded state which is represented with only one the salt-bridge partners charged (Eq. II).

Eq II: $$\Delta\Delta G_{dslv} = \Delta\Delta G_{folded,+} - \Delta\Delta G_{unfolded,+} + \Delta\Delta G_{folded,-} - \Delta\Delta G_{unfolded,-}$$

The $\Delta\Delta G_{brd}$ (bridge) is the electrostatic interactions between the salt-bridge partners. To calculate the bridge term only one calculation is needed, since the frc-mode in DelPhi was applied. In this calculation the frc-file contains the coordinate of one of the salt-bridge partners with the charged side chain atoms, while the pdb file contain the complete protein with the side chain of the other salt-bridge partner charged and the other residues uncharged. The $\Delta\Delta G_{prt}$ (protein) reflects the electrostatic energy between the charges in the salt-bridge and all the other atomic charges in the protein. Also here, only one run is needed when the frc-mode is applied. Then the side chain of the salt-bridge is charged in the frc-file and in the pdb-file all atoms are charged except the side chain atoms of the salt-bridge partners.

Result and discussion

Adaptation of enzymes to different environments occurs through mutations at specific positions in the protein sequence, resulting in enzymes capable of functioning in its specific habitat. Uracil DNA glycosylase from cod and human have been used as our model system to investigate the adaptation to low temperature. Inspection and comparison of their respective crystal structures shows differences in putative salt-bridges[27], but their possible role in providing stability has not yet been investigated. The crystallographic analysis of ion-pair interactions in cUDG and hUDG considered all histidines as protonated (charged), but NMR and previous computational investigations suggest that only His148 is charged[37]. Our simulations and subsequent analysis therefore only treat the His148 as charged, and the total number of ionic interactions is thus significantly lower than suggested by the crystallographic analysis[27]. The crystal structure of the psychrophilic enzyme (PDB entry 1OKB[27]) has 4 salt-bridges shorter than 5.0 Å, whereas the mesophilic homologue (PDB entry 1AKZ[26]) has 10 such salt-bridges (Table I). If we assume that salt-bridges are generally stabilizing, this implies that the mesophilic enzyme is far more stabilized when compared to its cold-active cousin. However, the situation is far more complicated. Several crystal structures of cUDG and hUDG have been determined and deposited to the protein data bank[48]. Five high resolution X-ray structures of hUDG have been examined, and their content of salt-bridges range from 5 to 10, while 4 and 6 are found in the two crystal structures of cUDG (Table I). Many ion-pairs are also located at the protein surface, and the electron density for highly solvent exposed lysines and arginines is often not well-defined. It should also be kept in mind that crystal structures present a static picture of the protein structures with one side-chain orientation for the partners in the salt-bridge, but with variability in the atomic positions as reflected in the crystallographic B-factors. Together, this adds even more complexity to the question of how important salt-bridges are to protein stability. It is clear that a much more reliable picture can be obtained by using computer simulations techniques. Molecular dynamics simulations allows for exploration of the conformational space of the protein and in particular of structural flexibility.

Ionic interactions present in the MD simulations

MD simulations generate an ensemble of conformations and thus include valuable information of the protein dynamics. The r.m.s.f. of the Cα atoms show that the MD simulations of both enzymes is equally stable throughout the simulation time (Fig. 1). In the

present simulations we have sampled conformations every ps yielding a total of 5000 structures for each enzyme that were analyzed with respect to possible salt-bridges interactions. The search for ion-pair interactions can be done in several different ways, but the distance between the two residues forming the ion pair is the first and most important criterion. Kumar and Nussinov[49] have suggested to differentiate between ion-pairs based on not only the distance between the charged-residue side-chain nitrogen and oxygen, but also the distance between the side-chain charged-group centroids[50]. Accordingly, an ion-pair is formed when both distances are less than 4.0 Å, a nitrogen-oxygen (N-O) bridge is formed when the distance between the atoms is less than 4.0 Å but with the centroid distance greater than 4.0 Å. Longer-range ion-pairs are formed when both distances are more than 4.0 Å. In this study we have used the distances between the following atoms: (Lys:Nζ, Arg:Cζ and His:Cε1) and (Asp:Cγ and Glu:Cδ). Fluctuations in the geometry of salt-bridges are observed in the trajectories where they break and reform. The distance between the residues in salt-bridges has been observed to vary in other MD simulation studies[51], NMR studies[52] and also between different crystal structures of the same protein[52]. Table I also shows that this is the case for UDG. The lifetime (or occupancy) of salt-bridges has therefore been used as the key parameter to identify ion pairs. It is defined as the number of structures where the salt-bridge is intact, judged by a distance criterion of 5 Å, divided by the total number of structures (5000). We require that salt-bridges must possess a lifetime greater than 30 % in order to be counted. Using this criterion, the distance between the salt-bridge partners is shorter than 5 Å for at least 30 % of the investigated structures, but the average distance calculated using all structures can be longer than 5 Å.

The environment of all charged amino acids was analyzed with respect to the presence of an oppositely charged amino acid in all sampled structures. If we require that the salt-bridge should possess a lifetime greater than 30 %, there is an increase in the number of salt-bridges in both cUDG and hUDG in the simulations as compared to the crystal structures (Table II). For cUDG seven new salt-bridges are formed during the MD simulations, while for hUDG one salt-bridge observed in the crystal structure disappears and three new are formed (Table II). The relatively higher increase in the number of salt-bridges between the crystal structure and the simulation for cUDG when compared to hUDG can be attributed to different crystallization conditions and particularly to the presence of PEG 4000 in hUDG and 1.4 M sodium citrate in cUDG[26,27]. The hydrophobic conditions in crystallization of hUDG may make it more energetically favorable for surface charges to interact with each

other, while high salt concentrations can lead to increased screening effects and solvent interactions for cUDG. cUDG and hUDG have a total of 11 and 12 salt-bridges that are intact for 30% of the simulation time, respectively (Table II). The average distance between the bridging residues from the MD simulations is 4.63 and 4.88 Å for cUDG and hUDG, respectively. Particularly stable ion-pairs are defined as those with a lifetime greater than 80 %. Table II shows that both cUDG and hUDG have six highly stable pairs, which also have the shortest average distance between the partners. The average distance is 4.06 and 3.93 Å for the six ion-pairs with lifetime > 80 % in cUDG and hUDG, respectively. All salt-bridges observed in the MD simulations are shown in Fig. 2A and B.

Electrostatic contribution to ion-pair stability.

One of the main objectives with this work is to investigate the role of ion-pairs in temperature adaptation of UDG. This requires that we are able to assess the strength of such interactions. We have combined MD simulations with continuum calculations for this purpose. Continuum electrostatics calculations have traditionally been carried out using static structural models, thus neglecting conformational fluctuations within salt-bridges and their interactions with explicit solvent. Full atomistic molecular dynamics simulations with explicit treatment of solvent represent a straightforward way of simultaneously including both effects. It is also possible to use rigorous statistical mechanics to extract thermodynamic information on salt-bridge formation, but these are generally more complicated to use compared to continuum models and requires more simulations time to reach convergence. Potential of mean force for association of ion pairs along user-defined paths has been computed[53], but application of artificial restraints to force association can be a limitation of such methods. Continuum methods based on classical electrostatics treat the solvent in terms of average bulk properties while the solute is represented in full atomic detail. Such methods have been widely used as both qualitative and quantitative tools in studies of electrostatic potentials, pH-dependent properties as well as solvation energies[54]. Ion-pairs and the electrostatic contribution to the free energy change upon salt-bridge formation have previously been investigated with continuum electrostatic calculations[17,20,22,23,47,49,52,55]. The computational method outlined by Hendsch and Tidor[47] has been followed here.

The electrostatic stability of all ion-pairs that survived in more than 30 % of the MD generated structures has been computed (Table II). In order to reduce the computing time only every 50th structure from the trajectories was included, and the calculations thus include 100 representative conformations for each ion-pair. The following energy terms are obtained:

the total electrostatic contribution to the free energy $\Delta\Delta G_{tot}$, the desolvation penalty for the charged residues $\Delta\Delta G_{dslv}$, the bridge energy for the electrostatic interaction between the pairing residues $\Delta\Delta G_{brd}$ and the protein energy term for the electrostatic interaction between the ion-pair and the surrounding protein environment $\Delta\Delta G_{prt}$. The $\Delta\Delta G_{ass}$ is the free energy change associated with forming a salt-bridge but it does not consider the interaction of the salt-bridge with the rest of the protein. $\Delta\Delta G_{ass}$ is the sum of the $\Delta\Delta G_{dslv}$ and the $\Delta\Delta G_{brd}$ [47].

The total electrostatic stability of an ion-pair is computed as the sum of $\Delta\Delta G_{dslv}$, $\Delta\Delta G_{brd}$ and $\Delta\Delta G_{prt}$, and these terms are the average values based on the 100 structures in our sub-set. To obtain the total electrostatic stability, 6 continuum electrostatic calculations are therefore needed, yielding a total of 600 for each of the pairs. While the folded state is modeled with all atoms present, the unfolded state is modeled using a single amino acid representation. How the three dimensional structure of proteins look like when they are unfolded is presently not known, which makes it very challenging to model the unfolded state. We have made attempts to use the structures from our high temperature unfolding studies of cUDG and hUDG[33], but obtaining convergent energies was extremely difficult (results not shown).

Effect of the internal dielectric constant and ionic strength.

Continuum electrostatic calculations have been shown to depend on the choice of the internal dielectric constant describing the macromolecular environment. Early calculations used a low dielectric constant, typically in the range 1-4, while more recent studies indicate that a larger constant is needed to reproduce experimental shifts in pK_a values[56,57]. The nature of the protein dielectric constant has been discussed extensively in the literature (see e.g. Warshel *et al.*[19]). van Vlijimen *et al.*[57] studied pK_a shifts using continuum calculations on 100 MD generated structures, and found that a protein dielectric constant of 20 resulted in best agreement with experimental data. It is not our intention to derive or find optimal values of this constant, but its effect on the strength of the ion pairs in UDG and on our results has, however, been assessed. In order to investigate how the protein dielectric constant (ε_p) affects the computed electrostatic interactions it assumes three different values: 4, 10 and 20. The results from these continuum calculations are summarized in Table III. The individual contributions from each ion-pair in all examined conditions are given in the Supplementary Material (Tables I-XII). Focusing on the $\Delta\Delta G_{tot}$ values presented in Table III, it is

immediately clear that increasing the dielectric constant in the protein effectively reduces the electrostatic stability of the ion-pairs. $\Delta\Delta G_{tot}$ is identical in cUDG and hUDG when ε_p=4, though with different individual contributions. The more favorable electrostatic interactions between the two partners ($\Delta\Delta G_{brd}$) and between the ion-pairs and the surroundings ($\Delta\Delta G_{prt}$) is outweighed by the higher desolvation penalty for cUDG as compared to hUDG (Table III). When the protein dielectric constant increases to 10 and 20, $\Delta\Delta G_{tot}$ becomes 0.5 kcal/mol more stabilizing in the cold-active enzyme at 298 K. The electrostatic stability is on average –2.3 and –2.1 kcal/mol with ε_p=4 for ion-pairs in cUDG and hUDG, respectively. The corresponding values with ε_p=10 are –1.6 and –1.5 kcal/mol and for ε_p=20 –1.4 and –1.2 kcal/mol for cUDG and hUDG respectively. We can use ±1.0 kcal/mol as a threshold to discriminate stabilizing pairs from those with small or negligible contributions. Among all the pairs, five have a stability of less than the threshold in hUDG while only one is observed in cUDG independent of the ε_p used. Thus, increasing the dielectric constant from 4 to 20 have negligible effect on the relative contribution of electrostatics in ion-pairs, and pairs with little or no effect from electrostatics is identified with all three ε_p.

Ionic strength (100 mM) does not affect the results appreciably and only serves to reduce the total stability, but not relatively between cUDG and hUDG. The total electrostatic contribution to the stability of the ion pairs is reduced by 1.1-1.2 kcal/mol with all three protein dielectric constants used. Presence of 100 mM salt decreases the desolvation penalty and the interaction between the ion pair and the rest of the protein, while the bridging term is increased (Table III). Others have also found that the ionic strength plays a minor role in relative values[47]. Ionic strength will of course play an important role when dealing with proteins that are exposed to extreme salinity (< 2 M)[58]. The enzymes studied here are also intracellular proteins and thus not exposed to extreme salinities. Since we are interested in the relative effect of ion-pairs between cUDG and hUDG, ionic strength will not be discussed in more detail.

Temperature and its effect on the electrostatic stability of ion-pairs.

Irrespective of the choice of ε_p comparable contributions to stability from salt-bridges are found in the two protein homologues at 298 K. The physical properties of water changes with temperature, and the dielectric constant of bulk water changes from 87.90 to 55.51 when the temperature is increased from 273 K to 373 K[17]. In order to investigate how the change in

dielectric properties of the solvent influence the stabilities, the calculations with ε_p=20 was reevaluated with ε_w=87.90 and 75.90 for cUDG and hUDG, respectively. Electrostatic interactions will accordingly become more favorable at higher temperatures due to this reduced screening effect, without considering other favorable or unfavorable contributions. The difference in the total electrostatic stability of ion pairs between cUDG and hUDG is largest with ε_p=10 and 20, and the results obtained with ε_p=20 are therefore expected to be valid for ε_p=4 and 10 as well. Table IV and V show the results from these calculations. The total electrostatic stability of the ion pairs is now approximately +3.1 kcal/mol more favorable in hUDG when compared to cUDG. The enhanced stability is almost exclusively attributed to differences in the bridging term, which is 3.6 kcal/mol more favorable in the mesophilic enzyme.

Location of ion pairs plays an important role in temperature adaptation.

Several different factors may influence the stability of ion-pairs, including the structural location, whether they are internal or external, local or global and the surrounding environment. The accessible surface area of the constituent residues has been calculated using a water probe of 1.4 Å[59] to discriminate between internal and external salt-bridges (Table II). If the average ASA of the two residues forming the pair is less than 20 % then the pair is classified as buried in the protein core (internal), otherwise they are defined as external. Only the conserved Glu112-Arg210 interaction is buried in cUDG and hUDG, and similar energetics is observed for this particular bridge (Table IV and V). The average ASA of all ion-pairs is 39 Å^2 and 50 Å^2 for cUDG and hUDG, respectively, and the desolvation penalty also reflects this fact (Table III, IV and V). The study of Hendsch and Tidor[47] suggest that ion pairs and hydrogen bonds destabilize the folded state due to loss of hydration at room temperature, an effect which is not fully compensated for by improved Coulombic interactions in the folded state. Our calculations show, however, that the desolvation penalty is compensated for by favorable Coulombic interactions in the folded state for most of the bridges in the two UDG enzymes (Table III). Only three ion pairs in hUDG have positive $\Delta\Delta G_{tot}$ when the internal dielectric constant is set to 4 (Supplementary Material, Table II), but $\Delta\Delta G_{tot}$ becomes negative for all three when ε_p is increased to 10 or 20. While the absolute value of all contributions to $\Delta\Delta G_{tot}$ is reduced when ε_p increases, Table III also shows that the $\Delta\Delta G_{dslv}$ is most affected.

Ion-pairs can be classified as either local or global depending on the number of residues that are between the two partners in the sequence. If five or less amino acids are between the two, the pair is regarded as local, otherwise a global bridge is formed. The psychrophilic enzyme has three salt-bridges between partners that are far apart in sequence (global salt-bridges) and all three link helices together. The mesophilic enzyme contains five global salt-bridges, the corresponding three observed in the psychrophilic enzyme and in addition two unique ones (Table II). The unique interactions are: Asp183-Lys302 and Glu197-Lys303. The majority of the ion-pairs are local (Table II), which is consistent with the general properties of salt-bridges in monomeric proteins[49]. These findings are also in agreement with the hierarchical view of how protein folding proceeds[60,61]. The energetics of local and global salt-bridges show an interesting trend, global bridges are more stabilized by electrostatics when compared to local. Global bridges have on average 0.3 to 1.5 kcal/mol more negative $\Delta\Delta G_{tot}$ values, and they are slightly more favorable in cUDG at 298 K. One of the two unique pairs observed in hUDG (Asp183-Lys302) is a highly stable salt-bridge, while the other (Lys197-Glu303) is destabilizing or weakly stabilizing. The three conserved pairs are of comparable stability in the cold- and warm-active UDG. If we take the respective physiological temperature into account, global ion-pairs are more stabilizing in hUDG while local pairs are of comparable stability (Table IV and V).

All but two salt-bridges in hUDG have a favorable interaction with the rest of the protein ($\Delta\Delta G_{prt}$, Supporting Material, Table II, IV and VI). The Lys197-Glu303 and Glu289-Lys293 are located at the protein surface and the side-chains extend into solution, which can explain the unfavorable $\Delta\Delta G_{prt}$. The local environment is generally more stabilizing in the psychrophilic enzyme regardless of the protein dielectric constant used. $\Delta\Delta G_{ass}$ which reflects the stability of ion-pairs in the absence of charges in the rest of the protein is more positive in cUDG when compared to hUDG. Together, this indicates more optimized dipoles and/or location of charges in the vicinity of ion-pair residues in cUDG[24]. Other studies have also shown that nearby charged residues can give rise to a strongly favorable $\Delta\Delta G_{prt}$ [23].

Putative ionic networks.

Our structural inspection revealed the presence of one ionic network in both hUDG and cUDG, each with three members (Table II). Networks of ionic interactions occur when more than two ionic residues interact, and an increased occurrence has been suggested to be

essential in explaining the enhanced thermal stability of thermophilic proteins[21,22]. Usher *et al.*[62] did not find a correlation between stability and the number of ion pairs when investigating the CheY protein. Lack of correlation between electrostatic contribution to the stability of hyperthermophilic proteins and the number of charged groups, ion pairs or ion pair networks was also observed by Xiao and Honig[22]. Location of the ionizable residues within the protein structures is, however, dictating whether or not specific interactions are stabilizing. Asp227 is interacting with Lys231 and Lys252 in cUDG (Fig. 3A) and their net electrostatic stability is –2.14 kcal/mol, while Lys302 interacts with Asp183 and Asp300 (Fig. 3B) with a net stability of –4.91 kcal/mol in hUDG (Table IV and V). The ionic network in hUDG is thus far more stabilizing than the one observed in cUDG, and this difference may be of structural importance. The network observed in hUDG appears to have a more important role, as it stabilizes the C-terminal (Fig. 3B), while the network in cUDG is between two helices.

Concluding remarks

We have here investigated the electrostatic stability of ion-pairs in the context of temperature adaptation of cold- and warm-active uracil DNA glycosylase by using MD simulations and continuum electrostatics calculations. The MD generated structural ensemble of cUDG differs significantly from the crystal structure with respect to the number of ion-pairs, which is primarily attributed to crystallization conditions. Seven new salt-bridges are formed during the simulations, while for its mesophilic counterpart only one more is found. Consequently, statistical analysis of the number of ion-pairs in crystal structures of proteins should be interpreted with care. Our comparison of crystal structures of UDG adds further support to this. It is not only lack of information on protein dynamics from crystal structures, but also effects from different crystallization conditions can cause differences in ion-pairs. Conformational ensembles obtained from NMR experiments have a significant degree of overlap with MD generated ensembles (see e.g. Kumar and Nussinov[52]), and NMR ensembles can give more information on protein dynamics.

The strength and the number of ion-pairs present in a protein and whether they are involved in networks or not are important for the overall structural stability. Their presence can have a large impact on the structural integrity modulating molecular plasticity. The main hypothesis for cold-adaptation is that increased structural flexibility is the cause of the

observed enhanced catalytic efficiency and reduced thermal stability of cold-active enzymes when compared to their warm-active cousins. Based on chemical intuition, ion-pairs should have a stabilizing effect on the protein and favor the folded state. Virtually all ion-pairs present in cUDG and hUDG have a favorable electrostatic contribution possibly leading to increased structural stability. When it comes to their net contribution to protein stability, entropy must also be considered. Strong interactions will reduce the available conformational space and the conformational entropy of the folded state will consequently decrease. Hence, ion-pairs destabilize the native state from an entropic point of view, whereas they are enthalpically stabilizing. The entropic effect is intrinsically difficult to estimate through computer simulations, and the fact that it changes with temperature makes it even more challenging to calculate. Enthalpic contributions also change with temperature, and we have investigated how the change in the solvent dielectric constant influences the stability of ion-pairs. Without taking the living temperature of the organisms into considerations, we find comparable electrostatic stability of ion-pairs in cUDG and hUDG. Proteins exhibit generally only marginal stability in their natural environment due to the delicate balance between stabilizing and destabilizing interactions. Medium sized globular proteins have average values for the Gibbs free energy of stabilization on the order of 50 kJ/mol[63], which is equivalent to only a small number of weak non-covalent interactions[11,12,64]. If we look at the respective environmental temperatures, the ion-pairs are more stabilizing in hUDG when compared to cUDG. The mesophilic enzyme also has more global bridges and a strong ionic network in the C-terminal, which may contribute to the enhanced thermal stability of hUDG.

Insight into the structural features promoting thermal stability is of great importance, particularly in design of enzymes with altered kinetic and thermodynamic properties. UDG from cod is presently commercialized, and its main application area is in PCR experiments removing contamination from previous PCR amplifications. cUDG is completely and irreversible inactivated by moderate heat treatment. The present study identifies some key residues involved in stabilization through ion pair network formation. In order to investigate the role of these in further detail mutagenesis combined with kinetic, thermodynamic and structural studies is needed.

Acknowledgement

Funding from the Research Council of Norway is gratefully acknowledged. The Norwegian Structural Biology Centre is supported by the Functional Genomics program (FUGE) of the Research Council of Norway.

References

1. Siddiqui KS, Cavicchioli R. Cold-adapted enzymes. Annu Rev Biochem 2006;75:403-433.
2. Smalås AO, Leiros HK, Os V, Willassen NP. Cold adapted enzymes. Biotechnol Annu Rev 2000;6:1-57.
3. D'Amico S, Collins T, Marx JC, Feller G, Gerday C. Psychrophilic microorganisms: challenges for life. Embo Rep 2006;7:385-389.
4. Gianese G, Bossa F, Pascarella S. Comparative structural analysis of psychrophilic and meso- and thermophilic enzymes. Proteins 2002;47:236-249.
5. Feller G. Molecular adaptations to cold in psychrophilic enzymes. Cell Mol Life Sci 2003;60:648-662.
6. Georlette D, Blaise V, Collins T, D'Amico S, Gratia E, Hoyoux A, Marx JC, Sonan G, Feller G, Gerday C. Some like it cold: biocatalysis at low temperatures. FEMS Microbiol Rev 2004;28:25-42.
7. Gerday C, Aittaleb M, Bentahir M, Chessa JP, Claverie P, Collins T, D'Amico S, Dumont J, Garsoux G, Georlette D, Hoyoux A, Lonhienne T, Meuwis MA, Feller G. Cold-adapted enzymes: from fundamentals to biotechnology. Trends Biotechnol 2000;18:103-107.
8. Russell RJM, Gerike U, Danson MJ, Hough DW, Taylor GL. Structural adaptations of the cold-active citrate synthase from an Antarctic bacterium. Structure 1998;6:351-361.
9. Bosshard HR, Marti DN, Jelesarov I. Protein stabilization by salt bridges: concepts, experimental approaches and clarification of some misunderstandings. J Mol Recognit 2004;17:1-16.
10. Jaenicke R. Protein Folding - Local Structures, Domains, Subunits, and Assemblies. Biochemistry 1991;30:3147-3161.
11. Jaenicke R. Stability and stabilization of globular proteins in solution. J Biotechnol 2000;79:193-203.
12. Dill KA. Dominant Forces in Protein Folding. Biochemistry 1990;29:7133-7155.
13. Pace CN. Polar group burial contributes more to protein stability than nonpolar group burial. Biochemistry 2001;40:310-313.
14. Brandsdal BO, Smalås AO, Åqvist J. Electrostatic effects play a central role in cold adaptation of trypsin. FEBS Lett 2001;499:171-175.
15. Gorfe AA, Brandsdal BO, Leiros HKS, Helland R, Smalås AO. Electrostatics of mesophilic and psychrophilic trypsin isoenzymes: Qualitative evaluation of electrostatic differences at the substrate binding site. Proteins: Struct, Funct, Genet 2000;40:207-217.
16. Moe E, Leiros I, Riise EK, Olufsen M, Lanes O, Smalas A, Willassen NP. Optimisation of the surface electrostatics as a strategy for cold adaptation of uracil-DNA N-glycosylase (UNG) from Atlantic cod (Gadus morhua). J Mol Biol 2004;343:1221-1230.

17. Kumar S, Nussinov R. Different roles of electrostatics in heat and in cold: Adaptation by citrate synthase. Chembiochem 2004;5:280-290.
18. Dominy BN, Minoux H, Brooks CL. An electrostatic basis for the stability of thermophilic proteins. Proteins 2004;57:128-141.
19. Warshel A, Sharma PK, Kato M, Parson WW. Modeling electrostatic effects in proteins. Bba-Proteins Proteom 2006;1764:1647-1676.
20. Elcock AH. The stability of salt bridges at high temperatures: Implications for hyperthermophilic proteins. J Mol Biol 1998;284:489-502.
21. Goldman A. How to make my blood boil. Structure 1995;3:1277-1279.
22. Xiao L, Honig B. Electrostatic contributions to the stability of hyperthermophilic proteins. J Mol Biol 1999;289:1435-1444.
23. Kumar S, Nussinov R. Relationship between ion pair geometries and electrostatic strengths in proteins. Biophys J 2002;83:1595-1612.
24. Hwang JK, Warshel A. Why Ion-Pair Reversal by Protein Engineering Is Unlikely to Succeed. Nature 1988;334:270-272.
25. Lindahl T, Nyberg B. Heat-Induced Deamination of Cytosine Residues in Deoxyribonucleic-Acid. Biochemistry 1974;13:3405-3410.
26. Mol CD, Arvai AS, Slupphaug G, Kavli B, Alseth I, Krokan HE, Tainer JA. Crystal-Structure and Mutational Analysis of Human Uracil-DNA Glycosylase - Structural Basis for Specificity and Catalysis. Cell 1995;80:869-878.
27. Leiros I, Moe E, Lanes O, Smalås AO, Willassen NP. The structure of uracil-DNA glycosylase from Atlantic cod (Gadus morhua) reveals cold-adaptation features. Acta Crystallogr D 2003;59:1357-1365.
28. Savva R, Mcauleyhecht K, Brown T, Pearl L. The Structural Basis of Specific Base-Excision Repair by Uracil-DNA Glycosylase. Nature 1995;373:487-493.
29. Ravishankar R, Sagar MB, Roy S, Purnapatre K, Handa P, Varshney U, Vijayan M. X-ray analysis of a complex of Escherichia coli uracil DNA glycosylase (EcUDG) with a proteinaceous inhibitor. The structure elucidation of a prokaryotic UDG. Nucleic Acids Res 1998;26:4880-4887.
30. Geoui T, Buisson M, Tarbouriech N, Burmeister WP. New Insights on the Role of the gamma-Herpesvirus Uracil-DNA Glycosylase Leucine Loop Revealed by the Structure of the Epstein-Barr Virus Enzyme in Complex with an Inhibitor Protein. J Mol Biol 2007;366:117-131.
31. Lanes O, Guddal PH, Gjellesvik DR, Willassen NP. Purification and characterization of a cold-adapted uracil-DNA glycosylase from Atlantic cod (Gadus morhua). Comp Biochem Physiol 2000;127:399-410.
32. Lanes O, Leiros I, Smalås AO, Willassen NP. Identification, cloning, and expression of uracil-DNA glycosylase from Atlantic cod (Gadus morhua): characterization and homology modeling of the cold-active catalytic domain. Extremophiles 2002;6:73-86.
33. Olufsen M, Brandsdal BO, Smalas AO. Comparative unfolding studies of psychrophilic and mesophilic uracil DNA glycosylase: MD simulations show reduced thermal stability of the cold-adapted enzyme. J Mol Graph Model 2006.
34. Olufsen M, Smalås AO, Moe E, Brandsdal BO. Increased flexibility as a strategy for cold adaptation - A comparative molecular dynamics study of cold- and warm-active uracil DNA glycosylase. J Biol Chem 2005;280:18042-18048.
35. Pearlman DA, Case DA, Caldwell JW, Ross WS, Cheatham TE, Debolt S, Ferguson D, Seibel G, Kollman P. Amber, a Package of Computer-Programs for Applying Molecular Mechanics, Normal-Mode Analysis, Molecular-Dynamics and Free-Energy Calculations to Simulate the Structural and Energetic Properties of Molecules. Comput Phys Commun 1995;91:1-41.

36. Wang JM, Cieplak P, Kollman PA. How well does a restrained electrostatic potential (RESP) model perform in calculating conformational energies of organic and biological molecules? J Comput Chem 2000;21:1049-1074.
37. Dinner AR, Blackburn GM, Karplus M. Uracil-DNA glycosylase acts by substrate autocatalysis. Nature 2001;413:752-755.
38. Jorgensen WL, Chandrasekhar J, Madura JD, Impey RW, Klein ML. Comparison of Simple Potential Functions for Simulating Liquid Water. J Chem Phys 1983;79:926-935.
39. Berendsen HJC, Postma JPM, Vangunsteren WF, Dinola A, Haak JR. Molecular-Dynamics with Coupling to an External Bath. J Chem Phys 1984;81:3684-3690.
40. Darden T, York D, Pedersen L. Particle Mesh Ewald - an N.Log(N) Method for Ewald Sums in Large Systems. J Chem Phys 1993;98:10089-10092.
41. Ryckaert JP, Ciccotti G, Berendsen HJC. Numerical-Integration of Cartesian Equations of Motion of a System with Constraints - Molecular-Dynamics of N-Alkanes. J Comput Phys 1977;23:327-341.
42. Vriend G. What If - a Molecular Modeling and Drug Design Program. J Mol Graph 1990;8:52-56.
43. Rocchia W, Alexov E, Honig B. Extending the applicability of the nonlinear Poisson-Boltzmann equation: Multiple dielectric constants and multivalent ions. J Phys Chem B 2001;105:6507-6514.
44. Rocchia W, Sridharan S, Nicholls A, Alexov E, Chiabrera A, Honig B. Rapid grid-based construction of the molecular surface and the use of induced surface charge to calculate reaction field energies: Applications to the molecular systems and geometric objects. J Comput Chem 2002;23:128-137.
45. Sitkoff D, Sharp KA, Honig B. Accurate Calculation of Hydration Free-Energies Using Macroscopic Solvent Models. J Phys Chem 1994;98:1978-1988.
46. Moreira IS, Fernandes PA, Ramos MJ. Accuracy of the numerical solution of the Poisson-Boltzmann equation. J Mol Struc-Theochem 2005;729:11-18.
47. Hendsch ZS, Tidor B. Do Salt Bridges Stabilize Proteins - a Continuum Electrostatic Analysis. Protein Sci 1994;3:211-226.
48. Bernstein FC, Koetzle TF, Williams GJB, Meyer EF, Brice MD, Rodgers JR, Kennard O, Shimanouchi T, Tasumi M. Protein Data Bank - Computer-Based Archival File for Macromolecular Structures. J Mol Biol 1977;112:535-542.
49. Kumar S, Nussinov R. Salt bridge stability in monomeric proteins. J Mol Biol 1999;293:1241-1255.
50. Barlow DJ, Thornton JM. Ion-Pairs in Proteins. J Mol Biol 1983;168:867-885.
51. Papaleo E, Olufsen M, De Gioia L, Brandsdal BO. Optimization of electrostatics as a strategy for cold-adaptation: A case study of cold- and warm-active elastases. J Mol Graph Model 2006.
52. Kumar S, Nussinov R. Fluctuations in ion pairs and their stabilities in proteins. Proteins: Struct, Funct, Genet 2001;43:433-454.
53. Masunov A, Lazaridis T. Potentials of mean force between ionizable amino acid side chains in water. J Am Chem Soc 2003;125:1722-1730.
54. Honig B, Nicholls A. Classical Electrostatics in Biology and Chemistry. Science 1995;268:1144-1149.
55. Lounnas V, Wade RC. Exceptionally stable salt bridges in cytochrome P450cam have functional roles. Biochemistry 1997;36:5402-5417.
56. Schutz CN, Warshel A. What axe the dielectric "constants" of proteins and how to validate electrostatic models? Proteins: Struct, Funct, Genet 2001;44:400-417.

57. van Vlijmen HWT, Schaefer M, Karplus M. Improving the accuracy of protein pK(a) calculations: Conformational averaging versus the average structure. Proteins: Struct, Funct, Genet 1998;33:145-158.
58. Elcock AH, McCammon JA. Electrostatic contributions to the stability of halophilic proteins. J Mol Biol 1998;280:731-748.
59. Lee B, Richards FM. Interpretation of Protein Structures - Estimation of Static Accessibility. J Mol Biol 1971;55:379-380.
60. Baldwin RL, Rose GD. Is protein folding hierarchic? II. Folding intermediates and transition states. Trends Biochem Sci 1999;24:77-83.
61. Tsai CJ, Kumar S, Ma BY, Nussinov R. Folding funnels, binding funnels, and protein function. Protein Sci 1999;8:1181-1190.
62. Usher KC, De la Cruz AFA, Dahlquist FW, Swanson RV, Simon MI, Remington SJ. Crystal structures of CheY from Thermotoga maritima do not support conventional explanations for the structural basis of enhanced thermostability. Protein Sci 1998;7:403-412.
63. Pfeil W. Protein Stability and Folding: A Collection of Thermodynamic Data. Berlin: Springer; 1998.
64. Jaenicke R. Protein Stability and Molecular Adaptation to Extreme Conditions. Eur J Biochem 1991;202:715-728.
65. Parikh SS, Mol CD, Slupphaug G, Bharati S, Krokan HE, Tainer JA. Base excision repair initiation revealed by crystal structures and binding kinetics of human uracil-DNA glycosylase with DNA. EMBO J 1998;17:5214-5226.
66. Parikh SS, Walcher G, Jones GD, Slupphaug G, Krokan HE, Blackburn GM, Tainer JA. Uracil-DNA glycosylase-DNA substrate and product structures: Conformational strain promotes catalytic efficiency by coupled stereoelectronic effects. Proc Natl Acad Sci U S A 2000;97:5083-5088.
67. Slupphaug G, Mol CD, Kavli B, Arvai AS, Krokan HE, Tainer JA. A nucleotide-flipping mechanism from the structure of human uracil-DNA glycosylase bound to DNA. Nature 1996;384:87-92.
68. DeLano WL. The PyMOL Molecular Graphics System: DeLano Scientific, San Carlos, CA, USA; 2002.

Tables

Table I
Salt-bridges and their distances[a] (Å) observed in crystal structures of cUDG and hUDG.

	cUDG	**V171E[b]**	**hUDG**	**E171V[c]**	**hUDG[d]**	**hUDG[d]**	**hUDG[d]**
PDB-code	1OKB	-	1AKZ	1YUO	1SSP	1EMJ	4SKN
Glu87-Lys90				4.30	3.78		4.06
Arg91-Glu92	4.39						
Glu96-Lys99	3.52	3.61	3.49	3.64	3.60	3.60	3.78
Glu111-Lys114			4.08			4.11	
Asp111-Arg115		4.36					
Glu112-Arg210	3.95	4.14	4.34	4.05	4.13	4.12	4.95
Asp133-Lys136				4.45			
Lys135-Asp136			4.85	3.86			
Lys138-Glu297		3.32					
Asp180-Lys/Arg282[e]		3.82	4.42	4.18	4.56	4.65	
Asp183-Lys302			4.16	4.28		4.94	5.00
Lys218-Glu219			4.63				
Asp227-Lys252	3.51	3.56	3.66	3.34	3.59	3.53	3.50
Asp257-Lys259							4.85
Asp257-Arg260						4.43	
Glu289-Lys293			4.34	4.25			
Asp300-Lys302			3.45	3.38			
Average distance	**3.84**	**3.80**	**4.14**	**3.97**	**3.93**	**4.20**	**4.36**
Number of salt-bridges	**4**	**6**	**10**	**10**	**5**	**7**	**6**

[a]The distances between the following atoms has been measured: (Lys:Nζ, Arg:Cζ and His:Cε1) and (Asp:Cγ and Glu:Cδ), and only pairs with a distance less than 5 Å is reported.

[b]cUDG with one mutant: V171E[16], no pdb code available

[c]hUDG with one mutant: E171V[16]

[d]hUDG in complex with different DNA fragments[65-67]

[e]Residue 282 is a Lys in cUDG and a Arg in hUDG.

Table II
Salt-bridges observed in the crystal structure and in the MD simulations[a] of cUDG and hUDG.

	cUDG				hUDG			
Salt-bridge	Cryst[b] (Å)	MD[b] (Å)	Occupancy[c] (%)	ASA[d] (Å^2)	Cryst[b] (Å)	MD[b] (Å)	Occupancy[c] (%)	ASA[d] (Å^2)
Glu87-Arg90	5.04	5.26	35	59				
Arg91-Glu92	4.39	4.36	92	46				
Glu96-Lys99	3.52	3.54	99	33	3.49	3.54	100	37
Glu111-Lys114					4.08	5.62	41	64
Asp111-Arg115	5.09	3.96	100	52				
Glu112-Arg210	3.95	3.99	100	16	4.34	4.02	100	19
Asp133-Lys135						6.33	40	55
Lys135-Asp136					4.85	-		
Asp136-Lys138	7.97	4.70	56	45				
Asp145-His148	7.10	5.35	65	29				
Asp180-Lys/Arg282*	5.03	4.26	82	30	4.42	4.32	99	31
Asp183-Lys302					4.16	3.85	90	51
Lys197-Glu303					12.60	6.32	36	58
Lys218-Glu219					4.63	4.81	60	65
Asp227-Lys231	5.24	5.82	49	45				
Asp227-Lys252	3.51	4.25	88	23	3.66	4.25	83	41
Asp257-Lys259	7.32	4.46	76	54	7.44	6.10	39	63
Glu289-Lys293					4.34	5.85	44	66
Asp300-Lys302					3.45	3.57	98	46
Average	5.29	4.63	77	39	5.12	4.88	69	50

[a]The MD distance is the average calculated using all simulated structures.

[b]The distances between the following atoms has been measured: (Lys:Nζ, Arg:Cζ and His:Cε1) and (Asp:Cγ and Glu:Cδ).

[c]Occupancy is percentage of the structures where the salt-bridge distance is less than 5 Å.

[d]Accessible surface area (ASA) is the accessible surface area calculated using a probe of 1.4 Å, and is the average of the two constituent residues.

Table III
Stabilities[a] of the salt-bridges observed in the MD simulations[b] of cUDG and hUDG

Protein	Salt (mM)	Dielec (prot)	$\Delta\Delta G_{dslv}$[c] kcal/mol	$\Delta\Delta G_{brd}$[d] kcal/mol	$\Delta\Delta G_{prt}$[e] kcal/mol	$\Delta\Delta G_{tot}$[f] kcal/mol	$\Delta\Delta G_{ass}$[g] kcal/mol
cUDG	0	4	71.1	-54.3	-42.5	-25.7	16.8
hUDG	0	4	58.5	-50.7	-33.5	-25.7	7.8
cUDG	0	10	29.6	-29.4	-18.1	-18.0	0.1
hUDG	0	10	24.5	-28.1	-13.9	-17.5	-3.6
cUDG	0	20	14.5	-20.2	-9.6	-15.3	-5.8
hUDG	0	20	12.2	-19.9	-7.1	-14.8	-7.7
cUDG	100	4	70.5	-51.5	-43.4	-24.4	19.0
hUDG	100	4	57.9	-47.6	-34.8	-24.5	10.3
cUDG	100	10	29.1	-26.8	-19.1	-16.8	2.3
hUDG	100	10	24.1	-25.2	-15.1	-16.3	-1.4
cUDG	100	20	14.1	-17.8	-10.6	-14.2	-3.6
hUDG	100	20	11.8	-17.1	-8.4	-13.7	-5.3

[a]The dielectric of the water was set to 80 in all calculations.

[b]The ion-pairs included in these calculations are given in Table 2, and their individual contributions are presented in the Supplementary material.

[c] $\Delta\Delta G_{dslv}$ is the desolvation penalty for the charged residues.

[d] $\Delta\Delta G_{brd}$ is the bridge energy for the electrostatic interaction between the pairing residues.

[e] $\Delta\Delta G_{prt}$ is the protein energy term for the electrostatic interaction between the ion-pair and the surrounding protein environment.

[f] $\Delta\Delta G_{tot}$ is the sum of these three terms.

[g] $\Delta\Delta G_{ass}$ is the sum of the $\Delta\Delta G_{dslv}$ and the $\Delta\Delta G_{brd}$.

Table IV

Average electrostatic free energy contributions[a] to salt-bridges[b] in cUDG at 273 K.

Salt-bridge	Occupied[d] %	ASA[e] Å^2	$\Delta\Delta G_{dslv}$[f] kcal/mol	$\Delta\Delta G_{brd}$[g] kcal/mol	$\Delta\Delta G_{prt}$[h] kcal/mol	$\Delta\Delta G_{tot}$[c,i] kcal/mol	$\Delta\Delta G_{ass}$[j] kcal/mol
Glu87-Arg90	35	59	0.74	-0.66	-0.98	-0.90 (0.37)	0.07
Arg91-Glu92	92	46	1.01	-1.81	-0.33	-1.13 (0.31)	-0.80
Glu96-Lys99	99	33	1.30	-1.99	-0.71	-1.41 (0.22)	-0.70
Asp111-Arg115	100	52	1.00	-1.96	-0.17	-1.12 (0.17)	-0.96
Glu112-Arg210	100	16	1.75	-2.60	-0.41	-1.26 (0.18)	-0.85
Asp136-Lys138	56	45	1.00	-1.22	-0.73	-0.94 (0.27)	-0.21
Asp145-His148	65	29	1.27	-1.58	-0.44	-0.76 (0.28)	-0.32
Asp180-Lys282	82	30	1.80	-1.76	-2.05	-2.01 (0.42)	0.04
Asp227-Lys231	49	45	1.00	-1.15	-1.06	-1.21 (0.38)	-0.15
Asp227-Lys252	88	23	1.56	-1.31	-1.18	-0.93 (0.37)	0.24
Asp257-Lys259	76	54	0.98	-1.65	-0.68	-1.35 (0.41)	-0.67
Sum	-	-	13.41	-17.70	-8.73	-13.03 (1.06)	-4.29
Average	77	39	1.22	-1.61	-0.79	-1.18 (0.31)	-0.39

[a]The dielectric constant of water and protein was 87.90 and 20, respectively.

[b]All salt-bridges that were inside a radii of 5 Å for 30 percent of the simulation time is included (Table 2).

[c]The standard deviations for the average values are indicated in parenthesis for the total energy.

[d]Occupancy is percentage of the structures where the salt-bridge distance is less than 5 Å.

[e]Accessible surface area (ASA) is the accessible surface area calculated using a probe of 1.4 Å, and is the average of the two constituent residues.

[f] $\Delta\Delta G_{dslv}$ is the desolvation penalty for the charged residues.

[g] $\Delta\Delta G_{brd}$ is the bridge energy for the electrostatic interaction between the pairing residues.

[h] $\Delta\Delta G_{prt}$ is the protein energy term for the electrostatic interaction between the ion-pair and the surrounding protein environment.

[i] $\Delta\Delta G_{tot}$ is the sum of these three terms.

[j] $\Delta\Delta G_{ass}$ is the sum of the $\Delta\Delta G_{dslv}$ and the $\Delta\Delta G_{brd}$.

Table V
Average electrostatic free energy contributions[a] to salt-bridges[b] in hUDG at 310 K.

Salt-bridge	Occupied[d] %	ASA[e] Å^2	$\Delta\Delta G_{dslv}$[f] kcal/mol	$\Delta\Delta G_{brd}$[g] kcal/mol	$\Delta\Delta G_{prt}$[h] kcal/mol	$\Delta\Delta G_{tot}$[c,i] kcal/mol	$\Delta\Delta G_{ass}$[j] kcal/mol
Glu96-Lys99	100	37	1.23	-2.34	-0.38	-1.50 (0.27)	-1.11
Glu111-Lys114	41	64	0.50	-1.20	-0.24	-0.94 (0.45)	-0.70
Glu112-Arg210	100	19	1.87	-3.02	-0.52	-1.67 (0.28)	-1.15
Asp133-Lys135	40	55	1.21	-1.49	-0.99	-1.28 (0.45)	-0.28
Asp180-Arg282	99	31	1.89	-2.48	-1.78	-2.37 (0.85)	-0.59
Asp183-Lys302	90	51	1.03	-2.04	-1.46	-2.47 (0.27)	-1.01
Lys197-Glu303	36	58	0.53	-1.01	0.10	-0.38 (0.42)	-0.48
Lys218-Glu219	60	65	0.53	-1.33	-0.01	-0.81 (0.42)	-0.80
Asp227-Lys252	83	41	1.29	-1.69	-0.11	-0.51 (0.42)	-0.39
Asp257-Lys259	39	63	0.78	-1.35	-0.71	-1.28 (0.42)	-0.57
Glu289-Lys293	44	66	0.47	-1.02	0.04	-0.50 (0.47)	-0.55
Asp300-Lys302	98	46	1.26	-2.33	-1.37	-2.44 (0.31)	-1.07
Sum	-	-	12.60	-21.30	-7.43	-16.13 (1.54)	-8.70
Average	69	50	1.05	-1.78	-0.62	-1.34 (0.42)	-0.73

[a]The dielectric constant of water and protein was 75.90 and 20, respectively.

[b]All salt-bridges that were inside a radii of 5 Å for 30 percent of the simulation time is included (Table 2).

[c]The standard deviations for the average values are indicated in parenthesis for the total energy.

[d]Occupancy is percentage of the structures where the salt-bridge distance is less than 5 Å.

[e]Accessible surface area (ASA) is the accessible surface area calculated using a probe of 1.4 Å, and is the average of the two constituent residues.

[f] $\Delta\Delta G_{dslv}$ is the desolvation penalty for the charged residues.

[g] $\Delta\Delta G_{brd}$ is the bridge energy for the electrostatic interaction between the pairing residues.

[h] $\Delta\Delta G_{prt}$ is the protein energy term for the electrostatic interaction between the ion-pair and the surrounding protein environment.

[i] $\Delta\Delta G_{tot}$ is the sum of these three terms.

[j] $\Delta\Delta G_{ass}$ is the sum of the $\Delta\Delta G_{dslv}$ and the $\Delta\Delta G_{brd}$.

Figures legends

Fig. 1

The r.m.s.f. of the Cα atoms as a function of time during the simulation of cUDG (grey) and hUDG (black).

Fig. 2

Salt-bridges present for more than 30 % of the MD generated structures of cUDG (A) and hUDG (B). The figure was generated using Pymol[68].

Fig. 3

The salt-bridge network in cUDG (A) and hUDG (B). The figure was generated using Pymol[68].

Figures

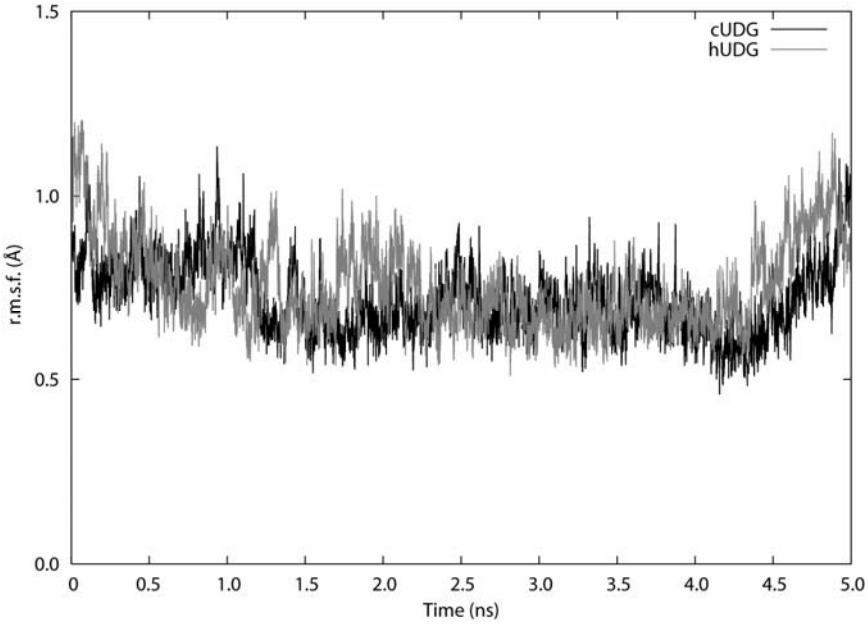

Fig. 1

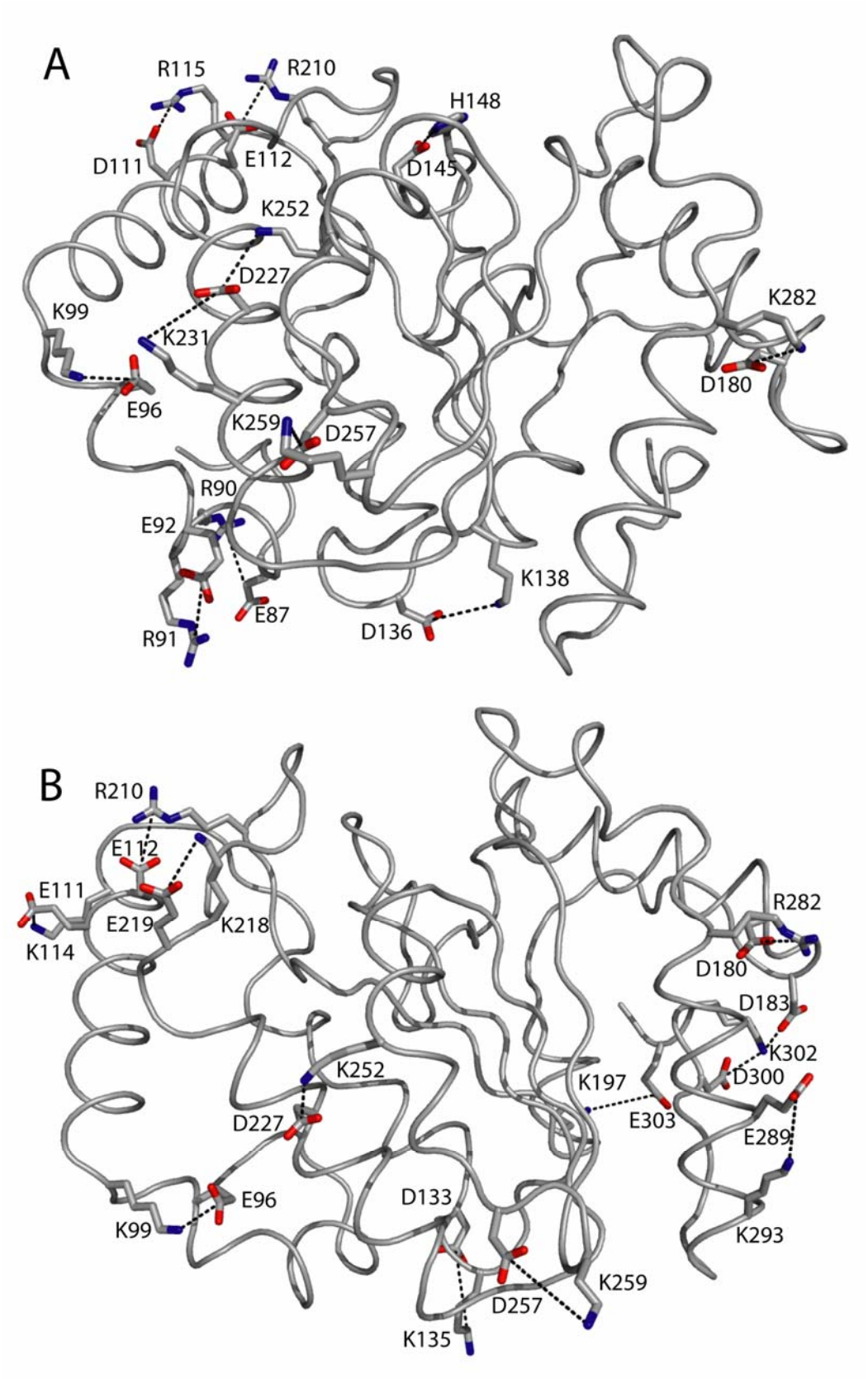
A
R115
R210
H148
D111
E112
D145
K252
D227
K282
K99
K231
E96
D180
K259
D257
R90
E92
K138
E87
R91
D136
B
R210
E112
E111
E219
K218
K114
R282
D180
D183
K302
K252
K197
D300
D227
E303
E289
E96
D133
K99
K293
K259
D257
K135

Fig. 2

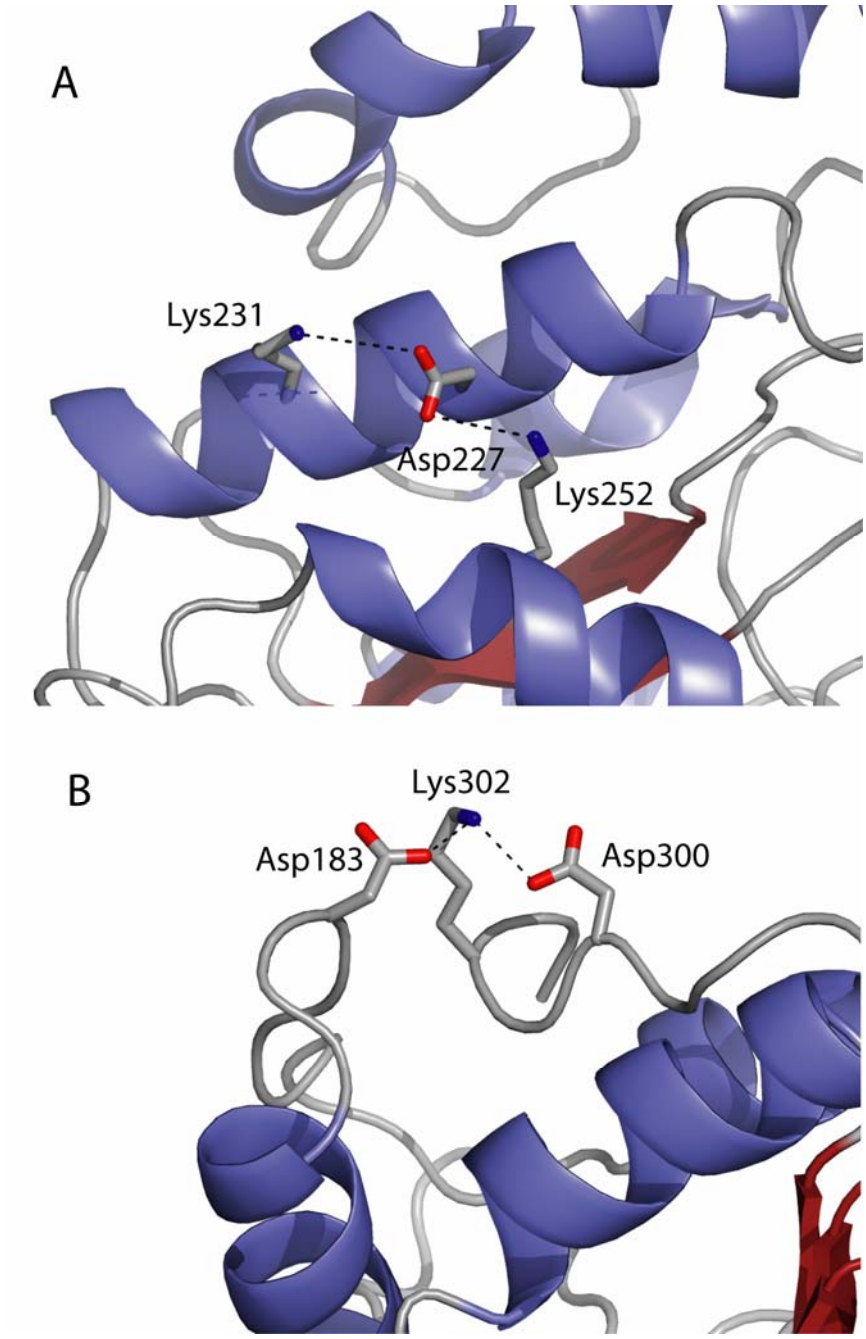

Fig. 3

Supporting information

Information for all the tables in supporting information. All salt-bridges that were inside a radii of 5 Å for 30 percent of the simulation time is included in the tables. The dielectric constant of water was set to 80. The standard deviations for the average values are indicated in parenthesis for the total energy. $\Delta\Delta G_{dslv}$ is the desolvation penalty for the charged residues, $\Delta\Delta G_{brd}$ is the bridge energy for the electrostatic interaction between the pairing residues, $\Delta\Delta G_{prt}$ is the protein energy term for the electrostatic interaction between the ion-pair and the surrounding protein environment and $\Delta\Delta G_{tot}$ is the sum of these three terms. $\Delta\Delta G_{ass}$ is the sum of the $\Delta\Delta G_{dslv}$ and the $\Delta\Delta G_{brd}$. Occupancy is percentage of the structures where the salt-bridge distance is less than 5 Å. Accessible surface area (ASA) is the accessible surface area calculated using a probe of 1.4 Å, and is the average of the two constituent residues.

Table I

Average electrostatic free energy contributions to salt-bridges in cUDG with $\varepsilon_p = 4$ and zero salt added.

Salt-bridge	**Occupied** %	**ASA** Å^2	**$\Delta\Delta G_{dslv}$** kcal/mol	**$\Delta\Delta G_{brd}$** kcal/mol	**$\Delta\Delta G_{prt}$** kcal/mol	**$\Delta\Delta G_{tot}$** kcal/mol	**$\Delta\Delta G_{ass}$** kcal/mol
Glu87-Arg90	35	59	3.97	-1.05	-4.55	-1.63 (1.23)	2.92
Arg91-Glu92	92	46	5.42	-5.87	-1.11	-1.56 (1.18)	-0.45
Glu96-Lys99	99	33	6.54	-5.93	-3.65	-3.04 (0.89)	0.61
Asp111-Arg115	100	52	5.72	-6.59	-1.13	-1.99 (0.73)	-0.87
Glu112-Arg210	100	16	9.85	-9.89	-2.86	-2.90 (0.87)	-0.04
Asp136-Lys138	56	45	4.65	-2.63	-3.03	-1.01 (0.96)	2.02
Asp145-His148	65	29	6.16	-5.09	-1.98	-0.91 (1.20)	1.08
Asp180-Lys282	82	30	10.81	-5.96	-10.77	-5.92 (1.96)	4.85
Asp227-Lys231	49	45	4.80	-2.85	-4.13	-2.18 (1.73)	1.95
Asp227-Lys252	88	23	7.83	-3.45	-5.80	-1.42 (1.51)	4.38
Asp257-Lys259	76	54	5.34	-4.96	-3.51	-3.12 (1.65)	0.38
Total		-	71.09	-54.26	-42.52	-25.7 (4.38)	16.83
Average	77	39	6.46	-4.93	-3.87	-2.34 (1.26)	1.53

Table II

Average electrostatic free energy contributions to salt-bridges in hUDG with $\varepsilon_p = 4$ and zero salt added.

Salt-bridge	Occupied %	ASA Å^2	$\Delta\Delta G_{dslv}$ kcal/mol	$\Delta\Delta G_{brd}$ kcal/mol	$\Delta\Delta G_{prt}$ kcal/mol	$\Delta\Delta G_{tot}$ kcal/mol	$\Delta\Delta G_{ass}$ kcal/mol
Glu96-Lys99	100	37	5.44	-5.53	-2.40	-2.49 (1.07)	-0.09
Glu111-Lys114	41	64	2.03	-2.14	-0.72	-0.82 (1.07	-0.10
Glu112-Arg210	100	19	9.53	-9.59	-2.83	-2.89 (1.14)	-0.06
Asp133-Lys135	40	55	5.61	-3.41	-5.38	-3.18 (1.21)	2.20
Asp180-Arg282	99	31	10.59	-7.81	-8.59	-5.81 (2.70)	2.78
Asp183-Lys302	90	51	4.87	-4.80	-4.58	-4.51 (0.96)	0.07
Lys197-Glu303	36	58	1.81	-1.57	0.01	0.25 (0.77)	0.25
Lys218-Glu219	60	65	1.99	-2.36	-0.57	-0.94 (0.94)	-0.37
Asp227-Lys252	83	41	5.42	-3.42	-1.52	0.47 (1.19)	1.99
Asp257-Lys259	39	63	3.56	-2.73	-2.74	-1.91 (1.15)	0.83
Glu289-Lys293	44	66	1.66	-1.55	-0.07	0.04 (0.92)	0.11
Asp300-Lys302	98	46	6.02	-5.80	-4.12	-3.90 (1.15)	0.22
Total	-	-	58.55	-50.71	-33.53	-25.7 (4.43)	7.84
Average	69	50	4.88	-4.23	-2.79	-2.1 (1.01)	0.65

Table III

Average electrostatic free energy contributions to salt-bridges in cUDG with $\varepsilon_p = 10$ and zero salt added.

Salt-bridge	Occupied %	ASA Å^2	$\Delta\Delta G_{dslv}$ Kkcal/mol	$\Delta\Delta G_{brd}$ kcal/mol	$\Delta\Delta G_{prt}$ kcal/mol	$\Delta\Delta G_{tot}$ kcal/mol	$\Delta\Delta G_{ass}$ kcal/mol
Glu87-Arg90	35	59	1.63	-0.87	-1.98	-1.22 (0.63)	0.76
Arg91-Glu92	92	46	2.23	-3.06	-0.57	-1.41 (0.56)	-0.84
Glu96-Lys99	99	33	2.80	-3.28	-1.51	-1.99 (0.41)	-0.49
Asp111-Arg115	100	52	2.28	-3.36	-0.42	-1.50 (0.33)	-1.08
Glu112-Arg210	100	16	3.98	-4.75	-1.06	-1.83 (0.37)	-0.77
Asp136-Lys138	56	45	2.08	-1.77	-1.43	-1.12 (0.65)	0.31
Asp145-His148	65	29	2.71	-2.72	-0.90	-0.91 (0.53)	-0.01
Asp180-Lys282	82	30	4.21	-3.05	-4.40	-3.23 (0.84)	1.16
Asp227-Lys231	49	45	2.11	-1.76	-1.97	-1.63 (0.75)	0.35
Asp227-Lys252	88	23	3.36	-2.08	-2.45	-1.17 (0.68)	1.28
Asp257-Lys259	76	54	2.18	-2.70	-1.46	-1.97 (0.75)	-0.52
Total		-	29.56	-29.41	-18.13	-17.99 (2.03)	0.15
Average	77	39	2.69	-2.67	-1.65	-1.64 (0.59)	0.01

Table IV

Average electrostatic free energy contributions to salt-bridges in hUDG with $\varepsilon_p = 10$ and zero salt added.

Salt-bridge	**Occupied** %	**ASA** Å^2	**$\Delta\Delta G_{dslv}$** kcal/mol	**$\Delta\Delta G_{brd}$** kcal/mol	**$\Delta\Delta G_{prt}$** kcal/mol	**$\Delta\Delta G_{tot}$** kcal/mol	**$\Delta\Delta G_{ass}$** kcal/mol
Glu96-Lys99	100	37	2.34	-3.10	-0.88	-1.64 (0.46)	-0.76
Glu111-Lys114	41	64	0.91	-1.38	-0.36	-0.84 (0.58)	-0.48
Glu112-Arg210	100	19	3.84	-4.61	-1.09	-1.87 (0.49)	-0.78
Asp133-Lys135	40	55	2.35	-1.94	-2.07	-1.66 (0.60)	0.42
Asp180-Arg282	99	31	4.07	-3.75	-3.43	-3.11 (1.29)	0.32
Asp183-Lys302	90	51	2.02	-2.68	-2.22	-2.88 (0.43)	-0.65
Lys197-Glu303	36	58	0.89	-1.12	0.04	-0.19 (0.47)	-0.23
Lys218-Glu219	60	65	0.93	-1.54	-0.16	-0.77 (0.53)	-0.61
Asp227-Lys252	83	41	2.42	-2.12	-0.48	-0.19 (0.58)	0.30
Asp257-Lys259	39	63	1.50	-1.65	-1.21	-1.36 (0.59)	-0.15
Glu289-Lys293	44	66	0.80	-1.11	0.01	-0.31 (0.56)	-0.32
Asp300-Lys302	98	46	2.49	-3.15	-2.03	-2.68 (0.51)	-0.65
Total	-	-	24.55	-28.14	-13.88	-17.5 (2.18)	-3.60
Average	69	50	2.05	-2.35	-1.16	-1.5 (0.59)	-0.30

Table V

Average electrostatic free energy contributions to salt-bridges in cUDG with $\varepsilon_p = 20$ and zero salt added.

Salt-bridge	**Occupied** %	**ASA** Å^2	**$\Delta\Delta G_{dslv}$** kcal/mol	**$\Delta\Delta G_{brd}$** kcal/mol	**$\Delta\Delta G_{prt}$** kcal/mol	**$\Delta\Delta G_{tot}$** kcal/mol	**$\Delta\Delta G_{ass}$** kcal/mol
Glu87-Arg90	35	59	0.79	-0.78	-1.08	-1.07 (0.42)	0.01
Arg91-Glu92	92	46	1.09	-2.07	-0.37	-1.35 (0.35)	-0.98
Glu96-Lys99	99	33	1.40	-2.28	-0.78	-1.65 (0.24)	-0.87
Asp111-Arg115	100	52	1.08	-2.23	-0.17	-1.33 (0.20)	-1.15
Glu112-Arg210	100	16	1.88	-2.92	-0.43	-1.48 (0.20)	-1.04
Asp136-Lys138	56	45	1.09	-1.41	-0.81	-1.13 (0.30)	-0.32
Asp145-His148	65	29	1.38	-1.80	-0.49	-0.91 (0.31)	-0.42
Asp180-Lys282	82	30	1.93	-2.00	-2.24	-2.31 (0.46)	-0.07
Asp227-Lys231	49	45	1.09	-1.33	-1.18	-1.42 (0.43)	-0.24
Asp227-Lys252	88	23	1.69	-1.51	-1.29	-1.12 (0.42)	0.18
Asp257-Lys259	76	54	1.06	-1.89	-0.75	-1.58 (0.46)	-0.83
Total		-	14.48	-20.23	-9.59	-15.34 (1.19)	-5.75
Average	77	39	1.32	-1.84	-0.87	-1.39 (0.34)	-0.52

Table VI

Average electrostatic free energy contributions to salt-bridges in hUDG with $\varepsilon_p = 20$ and zero salt added.

Salt-bridge	Occupied %	ASA Å^2	$\Delta\Delta G_{dslv}$ kcal/mol	$\Delta\Delta G_{brd}$ kcal/mol	$\Delta\Delta G_{prt}$ kcal/mol	$\Delta\Delta G_{tot}$ kcal/mol	$\Delta\Delta G_{ass}$ kcal/mol
Glu96-Lys99	100	37	1.19	-2.19	-0.37	-1.38 (0.26)	-1.00
Glu111-Lys114	41	64	0.48	-1.11	-0.23	-0.86 (0.42)	-0.63
Glu112-Arg210	100	19	1.81	-2.85	-0.50	-1.54 (0.27)	-1.03
Asp133-Lys135	40	55	1.17	-1.39	-0.96	-1.18 (0.42)	-0.22
Asp180-Arg282	99	31	1.84	-2.33	-1.71	-2.21 (0.80)	-0.50
Asp183-Lys302	90	51	1.00	-1.91	-1.38	-2.28 (0.26)	-0.91
Lys197-Glu303	36	58	0.51	-0.93	0.09	-0.33 (0.38)	-0.42
Lys218-Glu219	60	65	0.51	-1.23	-0.01	-0.73 (0.39)	-0.72
Asp227-Lys252	83	41	1.25	-1.57	-0.12	-0.45 (0.39)	-0.33
Asp257-Lys259	39	63	0.75	-1.26	-0.67	-1.18 (0.40)	-0.50
Glu289-Lys293	44	66	0.45	-0.94	0.04	-0.45 (0.43)	-0.49
Asp300-Lys302	98	46	1.22	-2.18	-1.29	-2.25 (0.29)	-0.96
Total	-	-	12.18	-19.88	-7.13	-14.84 (1.44)	-7.71
Average	69	50	1.01	-1.66	-0.59	-1.24 (0.39)	-0.64

Table VII

Average electrostatic free energy contributions to salt-bridges in cUDG with $\varepsilon_p = 4$ and 100 mM salt added.

Salt-bridge	Occupied %	ASA Å^2	$\Delta\Delta G_{dslv}$ kcal/mol	$\Delta\Delta G_{brd}$ kcal/mol	$\Delta\Delta G_{prt}$ kcal/mol	$\Delta\Delta G_{tot}$ kcal/mol	$\Delta\Delta G_{ass}$ kcal/mol
Glu87-Arg90	35	59	3.93	-0.80	-4.64	-1.51 (1.23)	3.13
Arg91-Glu92	92	46	5.38	-5.61	-1.05	-1.28 (1.17)	-0.24
Glu96-Lys99	99	33	6.47	-5.65	-3.71	-2.89 (0.88)	0.82
Asp111-Arg115	100	52	5.69	-6.34	-1.25	-1.90 (0.73)	-0.65
Glu112-Arg210	100	16	9.80	-9.64	-3.02	-2.86 (0.87)	0.16
Asp136-Lys138	56	45	4.58	-2.36	-3.10	-0.88 (0.96)	2.23
Asp145-His148	65	29	6.09	-4.85	-2.02	-0.78 (1.22)	1.24
Asp180-Lys282	82	30	10.77	-5.73	-10.90	-5.86 (1.96)	5.04
Asp227-Lys231	49	45	4.73	-2.58	-4.11	-1.97 (1.71)	2.14
Asp227-Lys252	88	23	7.75	-3.19	-6.02	-1.46 (1.51)	4.56
Asp257-Lys259	76	54	5.30	-4.70	-3.61	-3.01 (1.65)	0.60
Total		-	70.48	-51.45	-43.43	-24.40 (4.37)	19.03
Average	77	39	6.41	-4.68	-3.95	-2.22 (1.26)	1.73

Table VIII

Average electrostatic free energy contributions to salt-bridges in hUDG with $\varepsilon_p = 4$ and 100 mM salt added.

Salt-bridge	Occupied %	ASA Å^2	$\Delta\Delta G_{dslv}$ kcal/mol	$\Delta\Delta G_{brd}$ kcal/mol	$\Delta\Delta G_{prt}$ kcal/mol	$\Delta\Delta G_{tot}$ kcal/mol	$\Delta\Delta G_{ass}$ kcal/mol
Glu96-Lys99	100	37	5.38	-5.25	-2.54	-2.40 (1.07)	0.13
Glu111-Lys114	41	64	2.00	-1.89	-0.75	-0.64 (1.08)	0.11
Glu112-Arg210	100	19	9.47	-9.34	-2.96	-2.83 (1.14)	0.14
Asp133-Lys135	40	55	5.55	-3.16	-5.55	-3.15 (1.19)	2.39
Asp180-Arg282	99	31	10.55	-7.57	-8.67	-5.70 (2.65)	2.98
Asp183-Lys302	90	51	4.82	-4.54	-4.59	-4.30 (0.96)	0.28
Lys197-Glu303	36	58	1.75	-1.30	-0.10	0.35 (0.75)	0.45
Lys218-Glu219	60	65	1.94	-2.09	-0.72	-0.87 (0.92)	-0.15
Asp227-Lys252	83	41	5.34	-3.16	-1.72	0.47 (1.18)	2.19
Asp257-Lys259	39	63	3.53	-2.48	-2.86	-1.81 (1.16)	1.04
Glu289-Lys293	44	66	1.62	-1.29	-0.26	0.06 (0.85)	0.32
Asp300-Lys302	98	46	5.97	-5.54	-4.07	-3.64 (1.15)	0.44
Total	-	-	57.93	-47.61	-34.78	-24.46 (4.38)	10.32
Average	69	50	4.83	-3.97	-2.90	-2.04 (1.18)	0.86

Table IX

Average electrostatic free energy contributions to salt-bridges in cUDG with $\varepsilon_p = 10$ and 100 mM salt added.

Salt-bridge	Occupied %	ASA Å^2	$\Delta\Delta G_{dslv}$ kcal/mol	$\Delta\Delta G_{brd}$ kcal/mol	$\Delta\Delta G_{prt}$ kcal/mol	$\Delta\Delta G_{tot}$ kcal/mol	$\Delta\Delta G_{ass}$ kcal/mol
Glu87-Arg90	35	59	1.59	-0.62	-2.07	-1.11 (0.63)	0.97
Arg91-Glu92	92	46	2.19	-2.81	-0.51	-1.14 (0.55)	-0.62
Glu96-Lys99	99	33	2.74	-3.02	-1.57	-1.85 (0.39)	-0.28
Asp111-Arg115	100	52	2.25	-3.12	-0.54	-1.41 (0.33)	-0.87
Glu112-Arg210	100	16	3.94	-4.52	-1.21	-1.79 (0.37)	-0.58
Asp136-Lys138	56	45	2.03	-1.53	-1.52	-1.02 (0.46)	0.50
Asp145-His148	65	29	2.66	-2.51	-0.95	-0.80 (0.54)	0.14
Asp180-Lys282	82	30	4.17	-2.82	-4.53	-3.17 (0.83)	1.35
Asp227-Lys231	49	45	2.05	-1.52	-1.97	-1.43 (0.73)	0.54
Asp227-Lys252	88	23	3.30	-1.84	-2.66	-1.20 (0.69)	1.46
Asp257-Lys259	76	54	2.15	-2.46	-1.56	-1.86 (0.75)	-0.31
Total		-	29.09	-26.78	-19.08	-16.78 (1.96)	2.30
Average	77	39	2.64	-2.43	-1.73	-1.53(0.57)	0.21

Table X

Average electrostatic free energy contributions to salt-bridges in hUDG with ε_p = 10 and 100 mM salt added.

Salt-bridge	Occupied %	ASA Å^2	$\Delta\Delta G_{dslv}$ kcal/mol	$\Delta\Delta G_{brd}$ kcal/mol	$\Delta\Delta G_{prt}$ kcal/mol	$\Delta\Delta G_{tot}$ kcal/mol	$\Delta\Delta G_{ass}$ kcal/mol
Glu96-Lys99	100	37	2.29	-2.83	-1.01	-1.56 (0.45)	-0.54
Glu111-Lys114	41	64	0.88	-1.14	-0.39	-0.66 (0.59)	-0.27
Glu112-Arg210	100	19	3.80	-4.38	-1.23	-1.81 (0.49)	-0.58
Asp133-Lys135	40	55	2.30	-1.70	-2.24	-1.63 (0.58)	0.61
Asp180-Arg282	99	31	4.03	-3.52	-3.51	-3.00 (1.24)	0.51
Asp183-Lys302	90	51	1.99	-2.43	-2.24	-2.68 (0.43)	-0.44
Lys197-Glu303	36	58	0.84	-0.86	-0.07	-0.09 (0.44)	-0.03
Lys218-Glu219	60	65	0.88	-1.28	-0.30	-0.70 (0.52)	-0.40
Asp227-Lys252	83	41	2.37	-1.88	-0.67	-0.19 (0.57)	0.48
Asp257-Lys259	39	63	1.47	-1.41	-1.32	-1.26 (0.60)	0.06
Glu289-Lys293	44	66	0.76	-0.86	-0.17	-0.28 (0.49)	-0.11
Asp300-Lys302	98	46	2.45	-2.90	-1.99	-2.43 (0.51)	-0.45
Total	-	-	24.05	-25.21	-15.14	-16.29 (2.12)	-1.15
Average	69	50	2.00	-2.10	-1.26	-1.36 (0.58)	-0.10

Table XI

Average electrostatic free energy contributions to salt-bridges in cUDG with ε_p = 20 and 100 mM salt added.

Salt-bridge	Occupied %	ASA Å^2	$\Delta\Delta G_{dslv}$ kcal/mol	$\Delta\Delta G_{brd}$ kcal/mol	$\Delta\Delta G_{prt}$ kcal/mol	$\Delta\Delta G_{tot}$ kcal/mol	$\Delta\Delta G_{ass}$ kcal/mol
Glu87-Arg90	35	59	0.77	-0.55	-1.18	-0.96 (0.42)	0.22
Arg91-Glu92	92	46	1.06	-1.83	-0.33	-1.10 (0.34)	-0.77
Glu96-Lys99	99	33	1.37	-2.04	-0.84	-1.51 (0.23)	-0.68
Asp111-Arg115	100	52	1.06	-2.00	-0.29	-1.23 (0.19)	-0.94
Glu112-Arg210	100	16	1.85	-2.71	-0.58	-1.44 (0.20)	-0.86
Asp136-Lys138	56	45	1.06	-1.18	-0.91	-1.03 (0.29)	-0.13
Asp145-His148	65	29	1.34	-1.62	-0.55	-0.82 (0.32)	-0.27
Asp180-Lys282	82	30	1.90	-1.79	-2.37	-2.26 (0.46)	0.11
Asp227-Lys231	49	45	1.05	-1.11	-1.19	-1.25 (0.42)	-0.05
Asp227-Lys252	88	23	1.65	-1.30	-1.49	-1.14 (0.42)	0.35
Asp257-Lys259	76	54	1.04	-1.66	-0.85	-1.47 (0.46)	-0.62
Total		-	14.15	-17.79	-10.57	-14.21 (1.18)	-3.64
Average	77	39	1.29	-1.62	-0.96	-1.29 (0.34)	-0.33

Table XII

Average electrostatic free energy contributions to salt-bridges in hUDG with $\varepsilon_p = 20$ and 100 mM salt added.

Salt-bridge	Occupied %	ASA Å^2	$\Delta\Delta G_{dslv}$ kcal/mol	$\Delta\Delta G_{brd}$ kcal/mol	$\Delta\Delta G_{prt}$ kcal/mol	$\Delta\Delta G_{tot}$ kcal/mol	$\Delta\Delta G_{ass}$ kcal/mol
Glu96-Lys99	100	37	1.15	-1.94	-0.51	-1.30 (0.25)	-0.79
Glu111-Lys114	41	64	0.46	-0.87	-0.27	-0.69 (0.43)	-0.41
Glu112-Arg210	100	19	1.79	-2.63	-0.63	-1.48 (0.27)	-0.84
Asp133-Lys135	40	55	1.13	-1.17	-1.12	-1.16 (0.39)	-0.04
Asp180-Arg282	99	31	1.81	-2.12	-1.79	-2.10 (0.75)	-0.31
Asp183-Lys302	90	51	0.97	-1.67	-1.41	-2.11 (0.26)	-0.70
Lys197-Glu303	36	58	0.47	-0.70	-0.03	-0.25 (0.35)	-0.22
Lys218-Glu219	60	65	0.48	-0.99	-0.14	-0.65 (0.38)	-0.51
Asp227-Lys252	83	41	1.21	-1.36	-0.30	-0.45 (0.39)	-0.15
Asp257-Lys259	39	63	0.73	-1.03	-0.79	-1.08 (0.41)	-0.29
Glu289-Lys293	44	66	0.42	-0.70	-0.13	-0.41 (0.37)	-0.28
Asp300-Lys302	98	46	1.19	-1.95	-1.26	-2.02 (0.29)	-0.76
Total	-	-	11.82	-17.13	-8.39	-13.69 (1.38)	-5.31
Average	69	50	0.99	-1.43	-0.70	-1.14 (0.38)	-0.44